DOI 10.5162/sensor2017/A8.3

Investigation of bioreactors by instrumented flow-following sensor particles

Sebastian Felix Reinecke[1], Uwe Hampel[1,2]
[1] Helmholtz-Zentrum Dresden-Rossendorf, Bautzner Landstrasse 400, 01328 Dresden, Germany
[2] AREVA Endowed Chair of Imaging Techniques in Energy and Process Engineering, Technische Universität Dresden, 01062 Dresden, Germany
s.reinecke@hzdr.de

Abstract:
Instrumented flow-following sensor particles have been developed for investigation of hydrodynamic and biochemical processes chemical reactors and bioreactors, where standard measurement techniques are not applicable. The sensor particles allow autonomous long-term measurement of spatially distributed process parameters in the chemically and mechanically harsh environments of agitated industrial vessels. Each sensor particle comprises of an on-board measurement electronics that logs the signals of the embedded sensors. A buoyancy control unit enables automated taring to achieve neutral buoyancy of the sensor particles. Moreover, controlled floating of the sensor particles is possible to expose them for recovery from the fluid surface. The paper presents exemplary results from tests in an air-water column reactor, a pilot biogas digester and a waste water treatment plant.

Key words: sensor particle, autonomous sensor, flow follower, hydrodynamics, bioreactor.

Introduction

Advanced monitoring of the spatio-temporal distribution of process parameters in the large-scale vessels of chemical or bioreactors, such as industrial fermenters, biogas digesters and activated sludge basins, offers a high potential for the investigation and further optimization of plants and embedded processes. However, in most industrial scale applications the acquisition of these parameters and their spatial distributions in the large-scale vessels is hampered by the limited access to the process itself, because sensor mounting or cable connections are not feasible or desired. Therefore, state of the art instrumentation of such reactors is commonly limited to few spatial positions where it is doubtfully assumed that the measured parameters are representative for the whole reaction mixture.

Flow followers have always been in focus of chemical engineers for investigation of the complex hydrodynamic and biochemical processes in agitated reactor vessels beside the optical and tomographic ensemble measurement techniques [1]. Early concepts used visual observation of flow following rubber particles to study the circulation pattern of stirred tanks [2-3]. Later concepts allowed automatic detection of radio pills also in opaque mixed liquors of stirred bioreactor vessels [4-5].

Autonomous sensor technologies enable the design of embedded multi-parameter sensor-actuator systems with miniature size, low-power consumption, sufficient computational power and perspectively also wireless communication abilities for long-term monitoring of industrial processes. Thus, they are gaining increased attention in the process industry [6].

This paper presents selected results of applied instrumented flow-following sensor particles that have been designed for the specific use in industrial environments of multiphase process vessels. The applications involve typical bioreactor designs, namely an air-water column reactor, a pilot biogas digester and a waste water treatment plant (WWTP).

Sensor particle design and application

Instrumented flow-following sensor particles were developed by Thiele et al. [7] to capture the spatially distributed process parameters in the large-scale vessels of bioreactors. Data are transferred to an external computer system for further analysis after recovery from the process. The current configuration of the sensor particles comprises sensors for temperature, absolute pressure (immersion depth, axial position), 3D acceleration, 3D rotational rate and 3D magnetic field. The whole electronics is enclosed in a robust capsule (see fig. 1). Neutral buoyancy and free movement with the flow is guaranteed by the integrated buoyancy control unit [8]. The flow following characteristics for the macro-flow was validated

under realistic flow conditions and it is improved for increasing fluid viscosity [9].

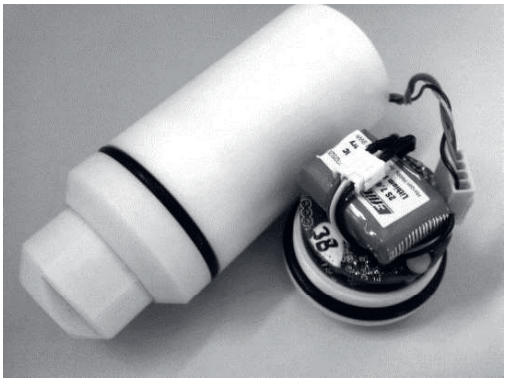

Fig. 1. Open sensor particle with connected electronics and piston of the buoyancy control unit.

Suspension in a pilot biogas digester

A study of a cylindrical pilot biogas digester was conducted with sensor particles to investigate the flow and particle suspension conditions (see fig. 2).The geometrical and fluid conditions are listed in table 1. A suspension of extruded straw fibres and water was used to simulate the typical non-Newtonian rheology of biogas substrates with resulting effective Reynolds numbers in the laminar region. The ratio of height to diameter is $H_0/D = 1.04$ which is favorable for best mixing efficiency. A central mixing unit with a pair of pitched blade impellers was used with off-bottom clearance C_1 and C_2 for sufficient suspension of particles. Two different impeller diameters were applied in trail A1 and A2 with a constant impeller tip velocity.

Tab. 1: Conditions of the hydrodynamic study in the biogas digester.

	parameter		trial A1	trial A2
fluid	*dry matter*	%	7	
	μ_{eff} (5 s^{-1})	Pa·s	1.5	
	ρ_f	$kg·m^{-3}$	1013	
	Re		<200	<300
	T	°C	31.8	29.9
vessel	H_0	m	1.04	
	D	m	1	
	V_V	m³	0.82	
impeller	type		pitched blade	
	blades		2	
	d	m	0.2	0.3
	C_1	m	0.2	
	C_2	m	0.7	
	n	s^{-1}	6.6	4.4
	v_{tip}	$m·s^{-1}$	4.1	
	P_{el}	W	370	360

The sensor particles were set to a measurement rate of $f_m = 10\ s^{-1}$ and resided for 42 min in the flow, i.e. $2.5·10^4$ measured values.

The normalized relative frequency $f_R(z/H_0)$ of the axial position *z* represents the axial residence profile of the sensor particles in the digester (see fig. 3). Moreover, the values of $f_R(z/H_0)$ reflect the particle concentration $\varphi_p(z/H_0)$ in the fluid since the sensor particles are considered as marker of the fluid elements itself. Thus, the axial residence profile delivers information about the axial particle distribution and also the suspension conditions.

Fig. 2. Pilot biogas digester.

Trial A1 shows an inhomogenous particle distribution with decreasing values f_R for $z/H_0 < 0.7$. The sensor particles mainly resided in the region of the upper impeller. That shows an unsufficient suspension power of the smaller impeller unit. In contrast, the profile is flattenend in trail A2 where the sensor particles were homogenously suspended in the digester. Only the regions $z/H_0 < 0.1$ close to the bottom and $z/H_0 > 0.9$ at the liquid surface were not entered by the sensor particles which might be caused by the apparent inertia of the sensor particles.

Assuming that the individual values f_R^i represent the axial particle distribution $\varphi_p(z/H_0)$ at the axial planes *i* with $i = 1…k$ the variance $s^2_{\varphi p}$ of the axial particle distribution is estimated according to (1).

$$\hat{s}^2_{\varphi p} = \frac{1}{k-1}\sum_{i=1}^{k}\left(f_R^i - 1\right)^2 \qquad (1)$$

A full suspension of particles is indicated by values of $s^2_{\varphi p} < 0.97$. Values of $s^2_{\varphi p} < 0.7$

indicate that the two-phase zone covers the whole volume. A homogeneous suspension is only present for values of $s^2_{\varphi p}$ < 0.5.

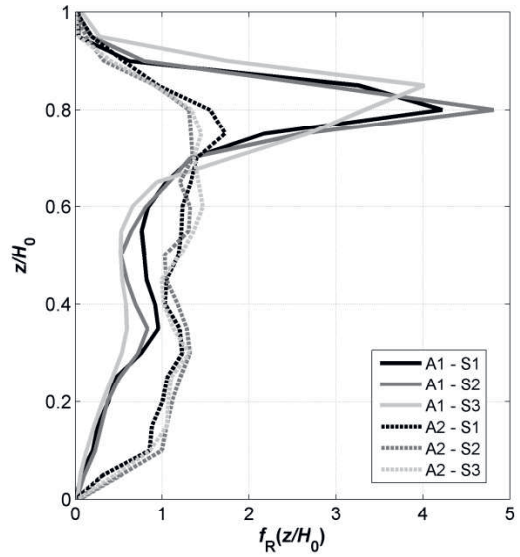

Fig. 3. Normalized relative frequency $f_R(z/H_0)$ of the axial position z of three sensor particles (S1, S2 and S3), i.e. the axial residence profile, in the digester for trial A1 and A2 (20 bins, width $\Delta z/H_0$ = 0.05).

Trial A1 shows values of $\hat{s}^2_{\varphi p}$ > 1.25 and thus the particle suspension is clearly insufficient (see tab. 2). The flat residence profile of trial A2 is reflected by the low values $\hat{s}^2_{\varphi p}$ < 0.26. In conclusion, a homogeneous particle suspension is achieved by chosing the impeller configuration of trial A2 with almost the same mixing power. Moreover, the mixing speed and power can still be reduced to meet the criterion of $\hat{s}^2_{\varphi p}$ = 0.5.

Tab. 2: Estimated variance $\hat{s}^2_{\varphi p}$ of the axial particle distribution for three sensor particles of trial A1 and A2.

sensor particle	1	2	3
A1	1.26	1.39	1.46
A2	0.25	0.23	0.26

Mixing in an air-water column reactor

Mixing in a lab-scale air-water column was investigated with sensor particles to proof the feasibility also in a gas liquid flow (see fig. 4). The column was operated as both bubble column (BC) and draft tube (DT) reactor (see tab. 3). It was aerated through a perforated plate at two different air flow rates. The sensor particles were set to a measurement rate of f_m = 4 s^{-1} and resided in the flow for 125 min and 83 min, i.e. $3{\cdot}10^4$ and $2{\cdot}10^4$ measured values, for Q_{air1} and Q_{air2}, respectively.

Tab. 3: Conditions of the air-water column reactor (BC: bubble column, DT: draft tube).

	parameter		BC	DT
fluid	T_{water}	°C	20.5	
	Q_{air1}	Nl/min	30	
	Q_{air2}	Nl/min	130	
column	H_0	m	2.5	
	D_i	m	0.392	
	V_C	m³	0.3	
draft tube	H_T	m		2
	D_a	m		0.28
	C_T	m		0.11

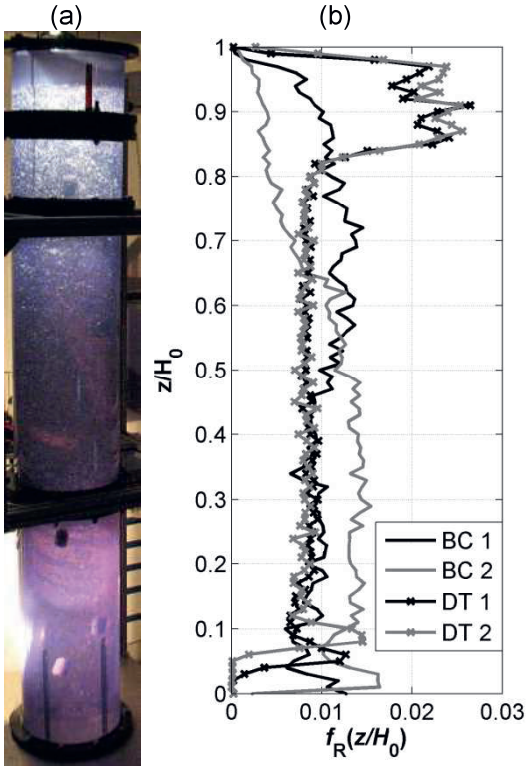

Fig. 4. (a) photograph of the air-water column reactor with the applied sensor particles and (b) normalized relative frequency $f_R(z/H_0)$ of the axial position z of a sensor particle in the air-water column reactor (BC: bubble column, DT: draft tube, 1: Q_{air1}, 2: Q_{air2}, 40 bins, width $\Delta z/H_0$ = 0.025).

The axial residence profiles of the sensor particle in fig. 4 show the varying homogeneity in the column depending on the reactor configuration and the air flow rate. The profile of DT is very homogenous along the height of the draft tube compared to the profile of BC. However, in the height above the draft tube there is an intense back mixing zone. The large recirculation zone is shifted from the upper to the lower part of the column for Q_{air2} in BC.

The impact of the draft tube to the axial flow can also be seen from the phase portrait of the

axial movement of the sensor particles (see fig. 5). Intense back mixing can be observed for BC from the circular trajectories in every axial position in the column. For DT there is clearly less dispersion and a main axial flow visible in the phase portrait, where only in upwards direction in the riser for $v_Z > 0$ few local circular trajectories are observed. Only in the region $z/H_0 > 0.85$ above the draft tube there is intense back mixing.

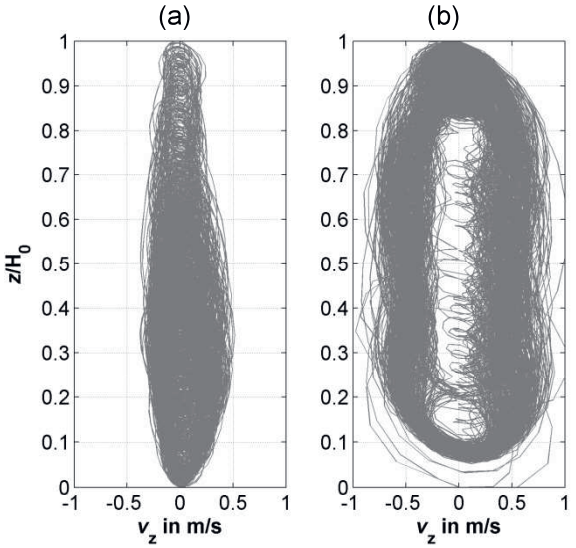

Fig. 5. Phase portrait of the axial movement of a sensor particle in the air-water column at Q_{air2}: (a) BC and (b) DT.

Mixing in the reactor can be further characterized by the liquid circulation time distribution. The liquid circulation time t_c is estimated by the return time of a sensor particle to the reference plane $z/H_0 = 0.5$ in the column (see fig. 6). The distribution for DT is very narrow compared to BC and it is shifted to smaller t_c for increased gas flow rate. This is also reflected by average $\bar{t}_c$ and the standard deviation σ_c of the circulation time distribution (see tab. 4). According to Luo and Al-Dahhan [11] these statistical quantities estimate the Peclét number according to (2).

$$Pe \approx 2 \cdot \left(\frac{\bar{t}_c}{\sigma_c}\right)^2 \quad (2)$$

The Peclét number is the ratio of the advective flow to diffusion and thus describes back mixing of mass transfer with $Pe = 0$ for ideal mixing and $Pe = \infty$ for ideal plug flow, i.e. convection and no back mixing. Accordingly, for BC the values of Pe are very low due to the intense back mixing flow (see tab. 4). In contrast, Pe significantly increased for DT due to the enforced axial flow direction.

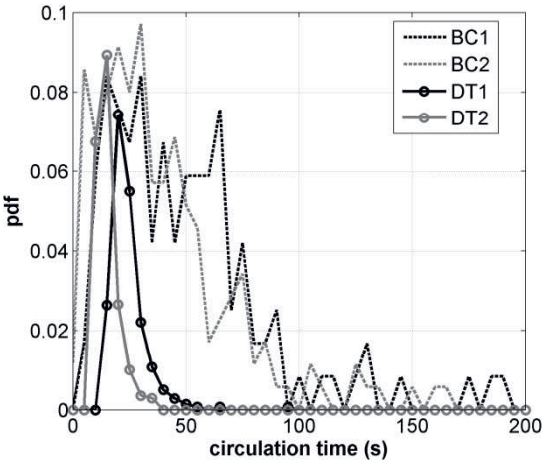

Fig. 6. Circulation time distributions of a sensor particle in the air-water column reactor (BC: bubble column, DT: draft tube, 1: Q_{air1}, 2: Q_{air2}, 40 bins, width $\Delta t = 5$ s).

Tab. 4: Average and standard deviation of the circulation time distribution of a sensor particle and estimated Peclét number in the air-water column reactor (BC: bubble column, DT: draft tube, 1: Q_{air1}, 2: Q_{air2}).

	BC 1	BC2	DT1	DT2
t_c	50.2	41.1	24.4	14.9
σ_c	36.4	35.7	8.3	5.1
Pe	3.8	2.7	17.2	17.0

Waste water treatment plant

Instrumented sensor particles were tested in an activated sludge basin at WWTP Großschweidnitz (see fig. 6). The reactor basin has a filling level of 5 m, a diameter of 23.4 m, i.e. a volume of 2077 m³. Intermittend aeration proceeds by 21 static plate diffusers with an aeration area of 42 m² on a sector of 45° at the bottom to provide oxygen for the nitrification phase. Two horizontal impellers are installed opposite in the basin to provide sufficient mixing energy.

Fig. 6. Activated sludge basin at WWTP Großschweidnitz (SOWAG mbH).

Automated taring of the sensor particles was conducted in a sample of the waste water (see

fig. 7) and they were set to a measurement rate of $f_m = 16\ s^{-1}$ and resided in the flow of the aerobic nitrification period for 43 min, i.e. $4.1 \cdot 10^4$ measured values. Final floating was initiated by the buoyancy control unit after the completed measurement and the sensor particles were recovered from the liquid surface (see fig. 7).

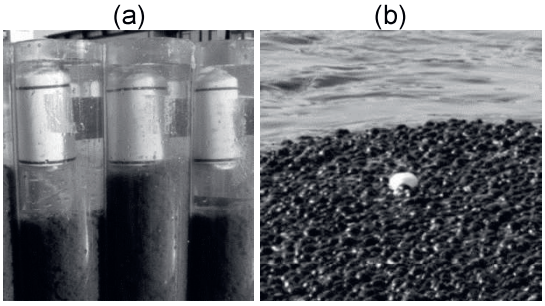

Fig. 7. Sensor particles at the WWTP: (a) during automated taring in a fluid sample and (b) after final floating at the liquid surface.

Analysis of the vertical movement of the sensor particles already gives important information about the flow in the basin, which can be seen from the phase portrait in fig. 8. The sensor particle movement covers the whole height of the basin which indicates an intense vertical mixing induced by the injected gas bubbles. The symmetry of the profile around $v_z = 0$ shows that the bubble induced circulation flow is also strong in downwards direction for sufficient oxygen mass transfer to unaerated zones in the basin. However, from fig. 8. it is obvious that v_z often exceeds the natural bubble rising velocity of $0.15 \ldots 0.3\ m \cdot s^{-1}$. This indicates a suboptimal interference of the impeller flow that decreases the bubble residence time and thus also the oxygen transfer efficiency.

The measured temperature in the basin is 16.9 °C in average and shows no relevant fluctuations. However, the filtered temperature signal of the sensor particles shows that small gradients can be detected by the flowing sensor particles (see fig. 9). The time series of temperature and vertical position in fig. 9 are correlated and reveal a dependency of the temperature on the vertical position in the basin. There is a delay of more than 100 s due to the limited response time of the integrated temperature sensor. However, this indicates existing temperature layers and local gradients.

Further analysis of the sensor particle movement and the fluid flow is enabled by the measured acceleration, angular rate and magnetic field. A sequence of this data is shown in fig. 10. The measured acceleration $\boldsymbol{a} = [a_x,\ a_y,\ a_z]$ shows that the sensor particle remains in its preferred z-upright orientation and higher fluctuations are present in x- and y-axis. Rotation around its axis is visible from the angular rate $\boldsymbol{\omega} = [\omega_x,\ \omega_y,\ \omega_z]$. At $t = 1535$ s the sensor particle resides at $z/H_0 = 0.4$ ($v_z \approx 0$), but it rotates very fast around its axial axis with $\omega_z > 200°\ s^{-1}$ which could be a sign for a local swirl. Also the measured magnetic flux $\boldsymbol{B} = [B_x,\ B_y,\ B_z]$ shows oscillations at $t = 1535$ s on the x- and y-axis, which indicates fast rotation of the sensor particle.

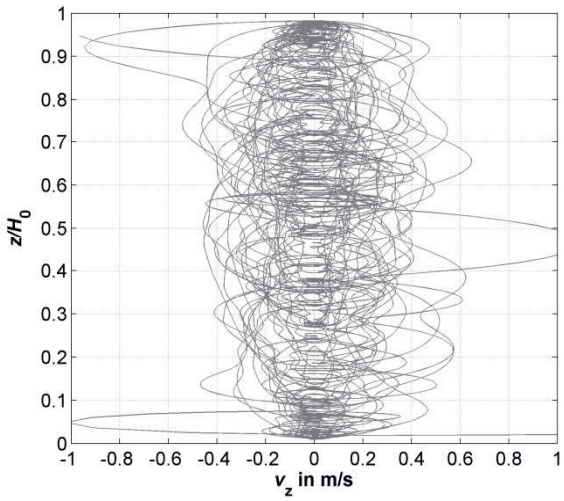

Fig. 8. Phase portrait of the axial movement of a sensor particle in the WWTP Großschweidnitz during nitrification.

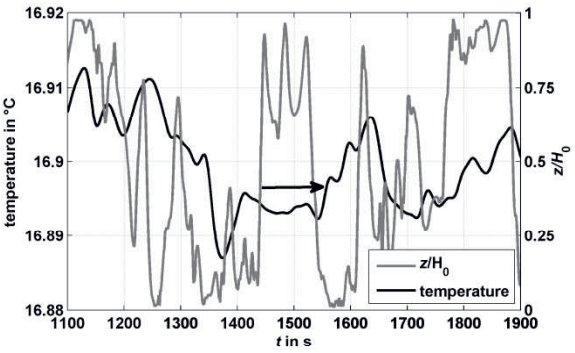

Fig. 9. Sequence of the filtered temperature signal of a sensor particle together with the vertical position in the WWTP.

All degrees of freedom of the sensor particle movement are captured by this measurement. This is the basis for passive movement tracking. Therefore suitable algorithms such as by Chambers et al. [10] will be considered in the future. Also external position markers may be included for improved performance of the position estimation [8].

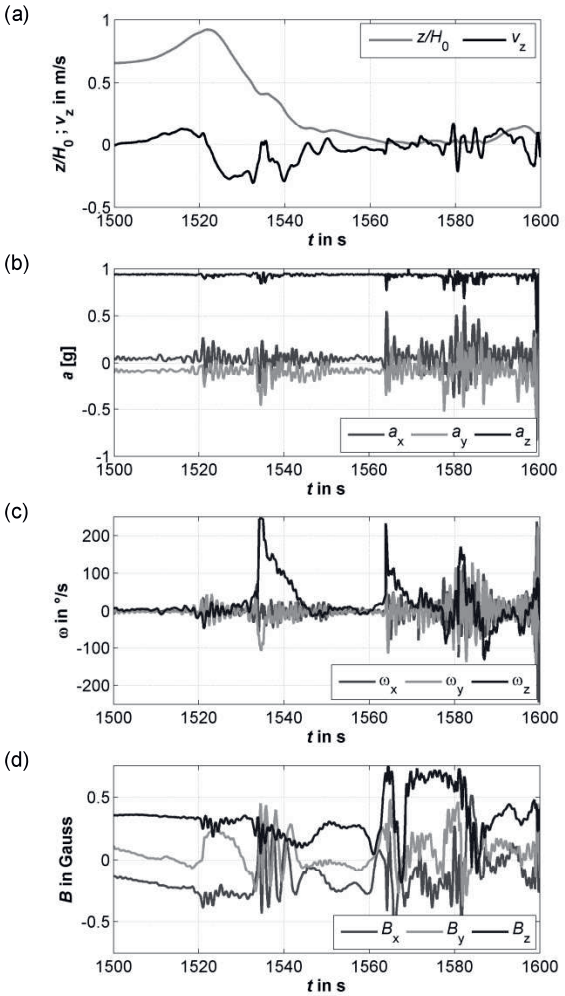

Fig. 10 Sequence of the measured movement data of a sensor particle in the WWTP Großschweidnitz: (a) vertical position z/H_0 and velocity v_z, (b) acceleration $\boldsymbol{a} = [a_x, a_y, a_z]$, (c) angular rate $\boldsymbol{\omega} = [\omega_x, \omega_y, \omega_z]$ and (d) magnetic flux $\boldsymbol{B} = [B_x, B_y, B_z]$.

Conclusion

Instrumented flow-following sensor particles were applied to typical bioreactor designs, namely an air-water column reactor, a pilot biogas digester and a WWTP. Taring, deployment and recovery of the sensor particles proceeded without difficulty due to the integrated buoyancy control unit.

The measured data reflect the process conditions in the reactor vessels. Analysis of the time series delivers important information about the flow behavior, mixing, particle suspension and thermal characteristics in the reactors.

Future work will encompass 3D reconstruction of the sensor particle position. Moreover, additional sensors may be included, e.g. for dissolved oxygen and pH.

Acknowledgements

Results from the WWTP Großschweidnitz do also originate from the research project LEOBEL which is funded by the German Federal Environmental Foundation (DBU - Deutsche Bundesstiftung Umwelt) under the reference number AZ30799. The experiment in the pilot biogas digester was conducted in cooperation with the Fraunhofer Institute for Ceramic Technologies and Systems Dresden (IKTS) at „Applikationszentrum Bioenergie Pöhl“.

References

[1] P. Mavros, Flow visualization in stirred vessels – A review of experimental techniques, Trans. I. Chem. E. 79, 113–127 (2001); doi: 10.1205/02638760151095926

[2] A. V. Porcelli, G. R. Marr, Propeller pumping and solids fluidization in stirred tanks, Ind. Eng. Chem. Fundamen.1(3), 172–179 (1962); doi: 10.1021/i160003a003

[3] I. Fořt, H. Valešová, V. Kudrna, Liquid circulation in a system with axial mixer and radial baffles, Collect. Czech. Chem. Commun. 36, 164-186 (1971).

[4] J. Bryant, Mixing in fermenters, Dissertation, University of Cambridge, UK, 1969.

[5] A. Day, Mixing in stirred tanks, Dissertation, University of Exeter, UK, 1975.

[6] M. Antoniou, M. C. Boon, P. N. Green, P. R. Green, T. A. York, Wireless sensor networks for industrial processes, Proceedings of IEEE SAS, New Orleans, LA, USA, 13–18 (2009); doi: 10.1109/SAS.2009.4801768

[7] S. Thiele, M. J. Da Silva, U. Hampel, Autonomous sensor particle for parameter tracking in large vessels, Meas. Sci. Technol. 21(8), 085201 1-8 (2010); doi: 10.1088/0957-0233/21/8/085201

[8] S. Reinecke, U. Hampel, J. Sens. Sens. Syst. 5, 213–220 (2016); doi: 10.5194/jsss-5-213-2016

[9] S.F. Reinecke, Instrumentierte Strömungsfolger zur Prozessdiagnose in gerührten Fermentern, Dissertation, Dresdner Beiträge zur Sensorik, Band 52, TUDpress, 2014.

[10] A. Chambers, et al., Robust Multi-Sensor Fusion for Micro Aerial Vehicle Navigation in GPS-Degraded/Denied Environments, American Control Conference 4-6 June 2014, 1892-1899, 2014.

[11] H.-P. Luo, M. H. Al-Dahhan, Macro-mixing in a draft-tube airlift bioreactor, Chem. Eng. Sci., 63, 1572-1585, 2008.